Research Article

SOHAG JOURNAL OF SCIENCES

https://doi.org/10.21608/sjsci.2023.222219.1094

# A Computational Intelligence Approach for Automatic Malignant Melanoma Diagnostics

Samy Bakheet[1], Mahmoud A. Mofaddel[1], and Aml El-Nagar[2,*]

[1] *Faculty of Computers and Artificial Intelligence, Sohag University, Sohag 82524, Egypt.*
[2] *Department of Mathematics, Faculty of Science, Sohag University, Sohag 82524, Egypt.*
[*] *E-mail: aml_saadeldin@science.sohag.edu.eg*

**Received:** 10th July 2023, **Revised:** 1st September 2023, **Accepted:** 5th September 2023
**Published online:** 25th September 2023

**Abstract**: Skin cancer is the most prevalent and perilous kind of cancer in human beings. Among the various types of dermatological malignancy, melanomas are particularly malignant and responsible for a significant number of cancer-related deaths. Early skin cancer detection plays a crucial role in reducing mortality rates and saving lives. So, Computer-Aided Diagnosis (CAD) systems that are driven by machine learning algorithms can help to detect melanoma early. In this article, we propose an innovative approach to melanoma recognition through the development of a fully automatic CAD system. To elevate the overall quality of input dermatoscopic images, we apply a series of preprocessing techniques such as median filtering and bottom-hat filtering. Besides that, an adaptive segmentation method based on the well-known Otsu thresholding technique is conducted to accurately extract suspected skin lesion regions from the improved input image. Then, we use the Local Binary Pattern (LBP) feature extraction method to characterize segmented skin lesions. This technique enables us to capture relevant information from the lesions effectively. Ultimately, the extracted features are inserted into a Decision Tree (DT) classifier to categorize each melanocytic cutaneous lesion in a given dermatoscopic image as either benign or melanoma. The proposed method is effectively tested and verified using a 10-fold cross-validation approach, achieving 90.35%, 88.47%, and 86.28% for average diagnostic accuracy, sensitivity, and specificity, respectively. The experimentation is conducted on the ISIC database, which contains suspect melanoma skin cancer cases, utilizing the MATLAB environment.
**Keywords:** Malignant Melanoma, Computer-Aided Diagnosis, Local Binary Pattern, Decision Tree.

## 1. Introduction

The skin serves as the first line of defense, creating a barrier between the body and its surrounding environment. It can feel pressure, pain, and temperature. The three main layers of skin are the epidermis, dermis, and hypodermis. In terms of frequency, skin cancer ranks as the highest prevalent among the cancers that impact the body, affecting over a million people worldwide each year [1]. There exist three principal categories of skin cancers: basal cell carcinoma (BCC), squamous cell carcinoma (SCC), and malignant melanoma where BCC and SCC have relatively lower mortality rates compared to malignant melanoma. In terms of skin malignancies, melanoma is a melanocyte cell cancer that typically develops in the epidermis. However, there are five stages in the progression of melanoma (ranging from stage 0 to stage 4) based on the extent of disease spread. Stage 0, also known as melanoma in situ, indicates that the melanoma cells are confined to the outer layer of the skin [1]. Stages 1 and 2 indicate the presence of melanoma cells in the layer beneath the epidermis, without spreading to lymph nodes or other body parts. Stage 3 involves cancer cell growth in the dermis layer, with nerve involvement. Stage 4 signifies metastasis to other organs, presenting significant treatment challenges (Figure 1).

As a result, early diagnosis greatly influences melanoma prognosis. It occurs more frequently in individuals with a history of sunburns, fair skin, overexposure to UV light, and use of tanning beds [2]. skin biopsy is the traditional and most accurate method of melanoma diagnosis. However, biopsy is an invasive, painful, costly, rigorous, and time-consuming technique.

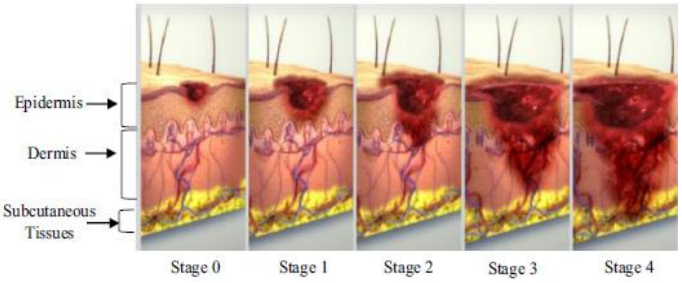


**Figure 1.** Stages of melanoma progression.

One of the most essential imaging techniques used for identifying and categorizing skin malignancies is dermatoscopy, also termed dermoscopy or epiluminescence microscopy (ELM), which is an alternative to biopsy. It makes the epidermis translucent by using either polarized light or liquid immersion. Therefore, it is used to support the conventional clinical diagnosis and to acquire images of skin lesions [3]. It enables dermatologists to differentiate between benign and malignant tumors, while also facilitating the early detection of melanoma by capturing the colors and morphological features of the skin. Images obtained through dermatoscopy are referred to as dermoscopic images.

On the other hand, the field of imaging-based computer-assisted diagnosis holds immense promise for the early detection and identification of malignant melanoma [4]. Dermatologists and healthcare providers utilize diverse approaches, incorporating the use of the ABCD rule [5], implementation of the Menzies Scoring method [6], and application of the Seven-Point Checklist [7], as part of their diagnostic processes for assessing the malignancy of skin lesions. At the core of these diagnostic methods and algorithms for pigmented skin lesions lies the morphologic diagnosis, which serves as a crucial element.

Despite the considerable progress achieved by diagnostic algorithms through simplified rules, there are still lingering challenges to overcome. In addition, the irregular shape and texture of skin lesions significantly contribute to misidentifications. Consequently, academics in the domains of computer vision and machine learning have actively developed various computerized diagnosis methods for detecting dermatological cancer [8]. Dermatologists highly value CAD systems as decision-making tools, which typically encompass four key phases: image data preprocessing, lesion segmentation, feature vector extraction, and feature classification. The initial phase solely requires capturing the image of the skin lesion. Subsequently, image pre-processing entails the elimination of noise, including salt-and-pepper noise, as well as other image artifacts, while enhancing the overall quality of the image. Following this, skin lesion segmentation is employed. The primary objective of this phase is to accurately delineate the boundaries of the skin abnormality from the adjacent unaffected skin, thereby isolating only the region of interest (ROI).

In order to precisely characterize a melanoma, a collection of pertinent dermatoscopic attributes is identified and extracted from the delineated lesion region. These features encompass attributes such as lack of symmetry, irregular borders, variations in color, and distinct structural characteristics, resembling the visual observations made by expert dermatologists. Subsequently, the extracted features are inserted into the classification phase, which classifies the cutaneous lesions into two categories: malignant and benign. This classification is based on a straightforward comparison of the feature values against predefined criteria.

The subsequent sections of our article are organized as outlined: The following section reviews prior research about the topic at hand. Section 3 elaborates on the proposed methodology, providing an overview of the general framework and specific details. Following that, Section 4 presents the experiments conducted and their corresponding evaluation findings, which are subsequently discussed. Lastly, Section 5 concludes the paper and outlines potential avenues for future research.

## 2. Related Work

Nowadays, computer technology has become prevalent as a decision support system in numerous medical domains, including skin cancer research. Consequently, computerized analysis techniques are employed on dermoscopy images to address various challenges, enabling dermatologists to make prompt and accurate diagnoses. To facilitate clinical diagnosis, a robust Computer-Aided Diagnosis (CAD) system has been created to distinguish between melanocytic and non-melanocytic skin lesions.

In [9], the author presented a technique for classifying and detecting melanocytic lesion by utilizing an SVM-based classification algorithm and an enhanced Histogram of Oriented Gradients (HOG) based skin lesion attributes. The experimental outcomes demonstrate promising classification performance, attaining a rate of accuracy at 97.32%, sensitivity at 98.21%, and specificity at 96.43%. In a separate study by Giotis et al. [10], a method for detecting malignant melanoma was proposed, which relies on skin digital images. This system utilizes three types of data, namely pigmentation of the lesion, textural characteristics of the lesion, and patient visual diagnostic attributes, to facilitate decision-making. The examining physician determines the existence or lack of a specific collection of visual characteristics, while color and texture attributes are automatically derived from the entire image. By employing a voting process that considers inputs from all three sources, the system establishes the ultimate classification decision for a given test condition.

In addition, in another recent study [11], the authors proposed a framework based on deep neural network (DNN) architecture to promptly and meticulously classify and grade dermatoscopic skin tumor images in real-time. This framework extracts a range of visual attributes grounded in the color and distinctive geometric characteristics of skin lesions. A rapid DNN classifier is then used to categorize the specified lesion features as either benign nevus or melanoma. The effectiveness of this approach was assessed using the publicly accessible PH2 dataset and achieved remarkable results of 97.5% accuracy, 96.67% sensitivity, and 100.0% specificity.

In another study, Bakheet and Al-Hamadi introduced an innovative computerized diagnostic system framework for identifying melanocytic malignancy in their publication [12]. Their framework incorporated an enhanced ensemble of Gabor-based descriptors and a rapid Neural Network classifier with multiple levels. To assess the effectiveness of their detection method, they conducted tests on the widely recognized PH2 benchmark dataset utilizing five-fold cross-validation. The outcomes indicated competitive performance, with accuracy, sensitivity, and specificity rates of 97.5%, 100%, and 96.87%, respectively. These findings highlight the framework's capability when compared to several existing state-of-the-art methodologies.

Furthermore, in [13], the authors presented a comprehensive computerized diagnostic system approach for fast and precise melanoma recognition in dermatoscopy images. The framework included preprocessing the input image for noise reduction and artifact removal. Skin lesions were described using an effective descriptor that combined HOG, LBP, N-LBP, and CS-HOG. Following the process of feature selection, the features were classified using Support Vector Machine (SVM), k-Nearest Neighbors (kNN), and Gentle adaboost (GAB) models to diagnose melanocytic

dermatological lesions as melanoma or benign. Experimental results on the MED-NODE dataset with 10-fold cross-validation demonstrated the framework's competitive or superior performance in comparison to several prevailing state-of-the-art approaches. The framework achieved high diagnostic metrics, including a ratio of accuracy at 94%, specificity at 92%, and sensitivity at 100%.

In another related work [14], a fully automated system is proposed for melanoma recognition, utilizing Support Vector Machines (SVMs) and an ensemble of distinct descriptors derived from the physical properties of skin lesions, including dissymmetry, edge irregularity, color diversity, diameter, and tissue lesion pattern. Additionally, in [15], various preprocessing methods are discussed, focusing on improving image quality, restoring damaged areas, and removing hair artifacts. Scaling and contrast stretching is used for enhancement, noise and blur reduction iareachieved through restoration techniques, and morphological techniques are employed for hair removal. Meanwhile, in [16], the researchers introduced an automatic method for segmenting Cutaneous lesion regions using GrabCut and k-means procedures. The effectiveness of the approach was assessed on the ISIC 2017 data repository and the public PH2 benchmark dataset, resulting in high accuracy values of 0.91935 and 0.96047, respectively.

In [17], the authors devised an algorithm for early identification and classification of skin tumors, specifically melanoma and non-melanoma types. The algorithm consisted of four processes: data pre-processing, ROI extraction, feature extraction, and classification. Data pre-processing involved median filtering and histogram equalization, followed by segmentation using Otsu's thresholding method. Features were extracted from the segmented image, including area, mean, variance, and standard deviation. These features were then inputted into classifiers such as k-Nearest Neighbor (kNN), Decision Tree (DT), Boosted Tree (BT), and Support Vector Machine (SVM). The article compared the accuracy of these classifiers, revealing that SVM achieved the best level of accuracy at 93.70%, followed by kNN at 92.70%, DT at 89.5%, and BT at 84.30%.

Murugan et al., [27] introduced an inventive methodology for melanoma recognition applying image analysis techniques. In the initial preprocessing step, they employed a median filter on the selected region and employed the mean-shift technique to segregate the isolated region. To capture essential attributes from the selected region, they utilized Invariant moments features like the Gray Level Run Length Matrix and Gray Level Co-occurrence Matrix (GLCM). For the classification of abnormal and normal cells, the authors employed support vector machines (SVM), probabilistic neural networks (NN), a and randomized ensemble of decision trees. The framework accomplished an accuracy of 89.00%. Additionally, in [31], the authors utilized a histogram normalization techtoder to improve chromatic contrast, while they also employed a dilation method to remove hair or skin defects from the images.

Thaajwer and Ishanka [29] utilized the ISIC database and attained an 85% accuracy level by employing the Otsu-based segmentation and Watershed-based method for image segmentation, along with Artificial Neural Networks (ANN), Support Vector Machines (SVM), and Convolutional Neural Networks (CNN) for image classification. Kassem et al., [28] utilized Google Net as a feature extraction technique and employed Multiclass SVM-based classification on the ISIC dataset, obtaining an 81% accuracy. Moreover, in [30], the researchers accomplished an 85.72% accuracy score through the use of the Watershed technique for segmenting images, implementing the ABCD criteria for feature extraction, and employing SVM, kNN, and RF for classifying data within the ISIC database.

## 3. Proposed Methodology

We present in this specific section a detailed synopsis of our proposed framework designed to automatically identify melanoma skin cancer by analyzing dermoscopy images. The framework follows a systematic automated diagnosis process that involves several steps, including image data preprocessing, lesion region extraction (segmentation), feature extraction, and classification. To aid in understanding the functioning of the proposed system, Figure 2 provides a simplified conceptual block diagram. This diagram serves as a visual representation, illustrating the essential components and the sequential flow of the framework. It effectively highlights the specific stages that are integral to the automated identification of melanoma skin cancer using dermoscopy images. By presenting this diagram, we visually emphasize the critical elements and the entirety of our proposed system's operation.

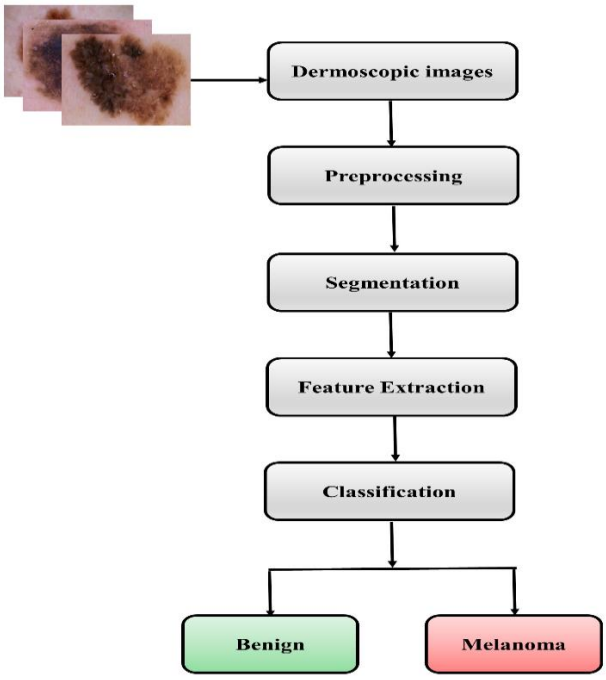


**Figure 2.** Diagrammatic depiction of our CAD framework for skin lesion recognition.

### 3.1. Image Data Preprocessing

The initial image data preprocessing stage, also known as data cleaning and preparation, plays a vital role in the establishment of a CAD system. Its primary purpose is to elevate the quality of cutaneous lesion images by reducing unwanted elements such as skin ridges, vessels, hairs, bubbles, reflections, ruler marks, ink marks, and black frames [18]. These artifacts can significantly hinder the segmentation of skin lesions. The preprocessing techniques employed include image resizing, conversion from RGB to Gray color space, noise removal, and hair removal. To remove noise from the images, a median filter with a window size of 7×7 is applied.

#### 3.1.1 Median Filtering

In our proposed approach, median filtering plays a vital role in enhancing input skin image quality, thereby strengthening the diagnostic model's effectiveness. Median filtering is a non-linear spatial technique in image processing that excels in noise and artifact removal [19]. Unlike mean filtering, which computes pixel averages, median filtering replaces pixel values with medians in a defined kernel, preserving edges and details while reducing outliers and noise. Due to the need for pristine images to diagnose malignant melanoma, which are susceptible to sensor noise and lighting variations, we employ median filtering as a pre-processing step to enhance image quality. This leverages median filtering's noise suppression while retaining essential image features, improving structural integrity. Our empirical results support its noise reduction efficacy without compromising image sharpness. This complements subsequent computational intelligence techniques, aiding precise malignant melanoma feature identification. The resultant heightened image quality significantly strengthens the diagnostic model's accuracy and robustness.

#### 3.1.2 Bottom-Hat Filtering

Additionally, for hair removal, morphological bottom-hat filtering is utilized.

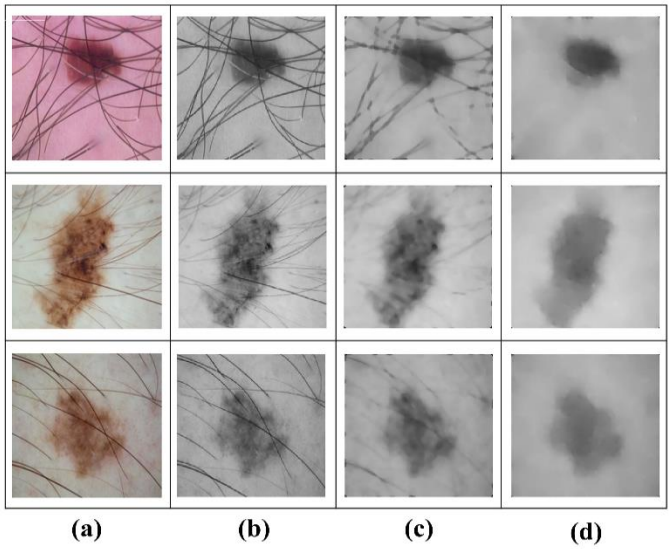


**Figure 3.** (a) Initial image, (b) Grayscale image, (c) Utilizing a median filtering process, and (d) Utilizing a bottom-hat filter.

This technique enhances dark spots against a white background. Subsequently, a closing operation is performed to eliminate any holes and fill them in the images. Figure 3 illustrates how the morphological processes, specifically median filtering, and bottom-hat filtering, effectively eliminate hair artifacts from dermoscopic images.

### 3.2. Lesion Region Extraction (Segmentation)

Cutaneous lesion region extraction is a technique used to separate the affected area from normal skin based on pixel homogeneity, aiming to simplify and transform the image representation for easier analysis. The process involves applying automatic thresholding, like Otsu's method of thresholding, to the individual red, green, and blue color channels, extracting the desired area from the image acquired from the preliminary preprocessing process [20]. By combining the binary masks obtained from each plane, a definitive lesion mask is generated, utilizing a three-channel masking approach to enhance segmentation accuracy. However, the partitioned image may have additional small-scale blobs unrelated to skin lesions. To address this, the morphological opening technique is applied to the output of a segmentation process [21]. Furthermore, the final segmented area, comprising solely the skin lesion, is obtained through the application of a smoothing process on the binary image using a recursive median filter technique with decreasing filter sizes (e.g., 7×7, 5×5, and 3×3). Additional measures, including two extra filters, are taken to prevent the preservation of extremely small non-cutaneous objects and ensure precise identification of desired cutaneous lesions. The process involves two phases: first, an adaptable morphological open-close filter eliminates extremely small objects while preserving the morphology and scale of larger objects; second, a "size filter" removes objects below a specified threshold size. To eliminate spurious artifacts smaller in size than 5% of the original image dimensions, experimental cleanup is performed on the binary image.

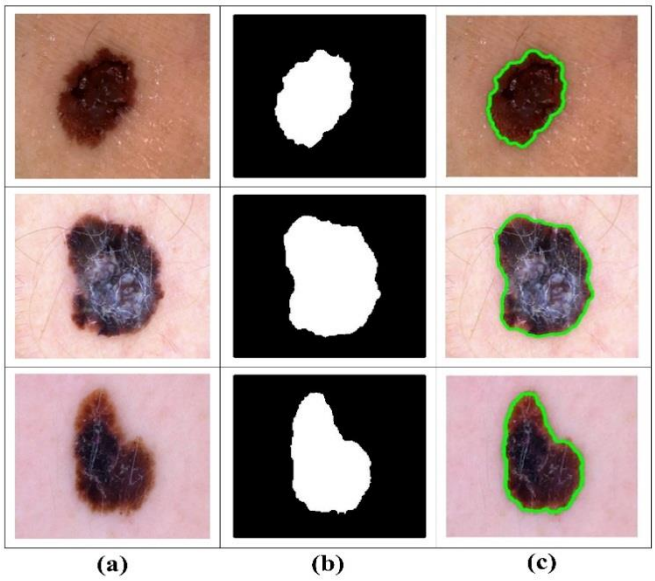


**Figure 4.** (a) Initial dermoscopy image, (b) Binarized mask, and (c) Traced pigmented skin abnormality.

Finally, after removing unnecessary image elements and isolated objects, Canny edge detection is applied to detect all image contours [22]. The results, as depicted in Figure 4, illustrate how the proposed segmentation procedure accurately differentiates the skin lesion from the adjacent healthy skin.

### 3.3. Feature Extraction

In the proposed CAD system, feature extraction is a crucial step involving the extraction of essential information from the input data. To achieve texture feature extraction, we employ the Local Binary Pattern (LBP) [23]. LBP is a specialized texture representation method that computes characteristics from the image by deriving binary numbers based on threshold values from neighboring pixels. This process results in an LBP descriptor that assigns decimal numbers to each pixel of the image, as demonstrated in Figure 5. Notably, LBP exhibits simplicity in computational capabilities and is adaptable to changes in the monotonic gray level. It operates in a block size of 3×3 pixels, where the values of neighboring pixels are compared to the central pixel. If a neighbor pixel's value is equal to or surpasses the central value, it is marked as one; in a contrasting case, it is marked as zero. These binary values are interconnected in a clockwise pattern, starting at the upper-leftmost neighbors of the center value, to form a new binary number. The resulting decimal value serves as an LBP code, effectively characterizing the respective pixel. From a more formal mathematical perspective, the mathematical description of Local Binary Patterns (LBP) can be expressed as follows:

$$LBP_{P,R(I_C,J_C)}=\sum_{p=0}^{p=1} s(x_p-x_c)2^p \quad (1)$$

where $x_p$, $x_c$ denote the central pixel of gray level, and $p$ neighboring pixels in the circle with radius $R$. The pixel value for all $x \geq 0$ is 1, and for all $x < 0$ is 0.

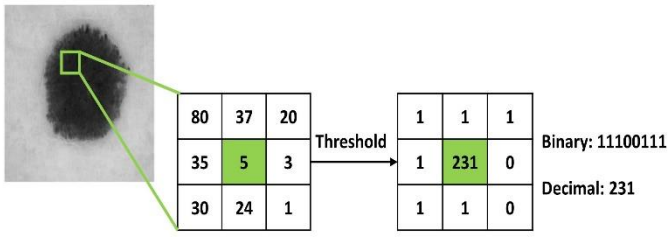


**Figure 5.** Basic LBP descriptor Process.

### 3.4. Feature Classification

The final step in CAD systems involves classifying melanoma as either benign or malignant based on extracted image features. This section encompasses a comprehensive elucidation of the classification model used in the proposed framework for skin cancer identification, which is based on the Decision Tree (DT) algorithm. The Decision Tree (DT) is a supervised machine learning technique introduced in [24] that effectively addresses both continuous and categorical problems. Its simplicity in design, effectiveness in decision-making, and ease of representation are widely recognized. Primarily used for classification, the DT algorithm can also be adapted for regression problems. By repeatedly partitioning the dataset into homogeneous subsets using a criterion that maximizes data separation, this algorithm constructs a tree-like structure. The key components of a basic DT include root, internal (or test), and leaf nodes. Split tests within internal nodes determine the final decisions for the target class at the leaf nodes. The leaf nodes either hold the target value or a probability vector indicating the outcome (benign or malignant).

## 4. Experimental Findings and Interpretation

Within this particular section, we present and discuss the experimental findings that exhibit the efficacy and performance of our recommended computational framework for pigmented skin lesion detection. To evaluate and validate the framework, we utilize a dermoscopic image dataset provided by the Kaggle repository, sourced from the ISIC Archive by the International Skin Imaging Collaboration [25]. This dataset encompasses a total set of 3297 dermatoscopic images in JPEG format. It consists of training and testing datasets for two categories of pigmented skin lesions: benign and malignant. The testing dataset encompasses 660 images sized at 224×244 pixels, while the training dataset encompasses 2637 images evenly distributed between the two categories to ensure equilibrium. To ensure computational efficiency, we first convert each skin lesion image in the dataset to grayscale and scale it down to a smaller size of 150×150 pixels for faster computation. We randomly split the pigmented lesion images in the dataset into two subsets, assigning 80% of the data for training purposes and reserving 20% for testing. Our proposed framework employs the ten-fold cross-validation strategy to enhance the level of accuracy in diagnosing within the dataset.

In addition to the above, we implement two preprocessing techniques, namely the median filter and bottom-hat filtering, to improve the effectiveness of the model. The segmentation method utilized to isolate the region of concern from the whole image is the Otsu approach. As shown in Figure 6, we provide a selection of skin lesion images sourced from the Kaggle database.

**Figure 6.** A selection of skin lesion images sourced from the Kaggle database: malignant lesions (rows 1 and 2) versus benign lesions (rows 3 and 4).

The efficacy of the proposed model is evaluated utilizing three assessment criteria: Accuracy (AC), Sensitivity (SN), and Specificity (SP). These criteria are defined as follows:

Accuracy: evaluates the holistic efficacy of the system, guaranteeing precise outcomes to mitigate the occurrence of incorrect diagnosis. It is determined using a mathematical Equation. (2).

$$\boldsymbol{Accuracy}\ (\%) = \frac{TP + TN}{TP + TN + FP + FN} \times 100 \qquad (2)$$

Sensitivity: indicates the system's ability to identify individuals with the disease, with higher values indicating better detection. It is determined using a mathematical Equation. (3).

$$\boldsymbol{Sensitivity}\ (\%) = \frac{TP}{TP + FN} \times 100 \qquad (3)$$

Specificity: signifies the system's capacity to correctly identify individuals without the disease, with higher values indicating better identification of healthy individuals. It is determined using a mathematical Equation. (4).

$$\boldsymbol{Specificity}\ (\%) = \frac{TN}{TN + FP} \times 100\% \qquad (4)$$

where,

**TP** (True Positive rate): represents cases that are expected to belong to the positive class.

**TN** (True Negative rate): represents cases that are expected to belong to the negative class.

**FP** (False Positive rate): refers to cases that are incorrectly classified as positive, even though they belong to the negative class.

**FN** (False Negative rate): refers to cases that are incorrectly classified as negative, even though they belong to the positive class.

In order to gauge the effectiveness of our suggested model, we conducted a comprehensive assessment, measuring its accuracy, sensitivity, and specificity. The results showed impressive average rates of 90.35%, 88.47%, and 86.28% respectively. Additionally, to fairly evaluate the competitiveness of our model, we conducted a comparative experiment against various state-of-the-art baselines. Our primary focus was on the accuracy of melanoma detection, and we utilized the publicly available ISIC dataset for this purpose. The summarized comparison in Table 1 confirms that the proposed framework delivers better results when compared to alternative advanced approaches.

The proposed model was executed using MATLAB software (version R2019a) on a Windows 10 Professional 64-bit operating system. The implementation was performed on a PC equipped with an Intel(R) Core(TM) i7 CPU running at 2.60 GHz and 8GB RAM.

**Table 1.** Comparison of qualitative performance between the proposed methodology and various alternative advanced approaches.

| Approach | Accuracy (%) |
|---|---|
| **Our Model** | **90.35** |
| Murgan et al. (2021) [27] | 89.00 |
| Kassem et al. (2020) [28] | 81.00 |
| Thaajwer & Ishanka (2020) [29] | 85.00 |
| Murugan et al. (2019) [30] | 85.72 |
| Carrera & Dominguez (2019) [31] | 75.00 |

## 5. Limitations

Our proposed computational intelligence approach exhibits promising strides in automating the diagnosis of malignant melanoma. However, it's vital to recognize a range of limitations that demand careful consideration. These constraints not only shed light on the encountered challenges but also serve as a foundation for future investigations aimed at honing the precision and efficacy of our diagnostic system, with the potential to enhance patient care and outcomes. Among the challenges and limitations are: low contrast between lesion and surrounding skin, variations in lesion shape and texture, unclear lesion borders, inconsistent color distribution within lesions, presence of marginal features like dark corners, and the interference of noise artifacts such as hair, gel, scars, pen marks, oil drops, and ruler signs, necessitating the implementation of robust noise-handling techniques.

## 6. Conclusion and Future Directions

The occurrence of malignant melanoma has seen a rapid rise in recent decades, leading to a growing interest in automated melanoma detection from pigmented dermoscopic images as a means to avoid invasive biopsies. This study presents a method for identifying melanoma skin cancer by analyzing images of affected skin areas. To effectively distinguish between malignant and benign skin lesions in dermoscopic images, a Decision Tree (DT) classifier is utilized. The experimental findings on the ISIC dermoscopy imaging database, which is openly accessible, reveal that the suggested framework exhibits superior performance when compared to other cutting-edge methods. It achieves an average accuracy rate of 90.35%, sensitivity rate of 88.47%, and specificity rate of 86.28%, further demonstrating its effectiveness. Therefore, this proposed system holds great promise as a valuable clinical tool for physicians, aiding them in the accurate and efficient diagnosis of melanoma skin cancer. Future research directions involve exploring deep learning techniques to further enhance the accuracy of our system and ensure compliance with clinical requirements for widespread adoption.

## CRediT authorship contribution statement:

Conceptualization, Samy Bakheet.; methodology, Samy Bakheet, and Aml El-Nagar.; software, Samy Bakheet, and Aml El-Nagar.; validation, Samy Bakheet, and Mahmoud A. Mofaddel.; formal analysis, Samy Bakheet, and Mahmoud A. Mofaddel.; investigation, Samy Bakheet and Mahmoud A. Mofaddel.; resources, Aml El-Nagar.; data curation, Samy Bakheet, and Aml El-Nagar.; writing—original draft preparation, Aml El-Nagar.; writing—review and editing, Aml El-Nagar.; visualization, Samy Bakheet.; supervision, Samy Bakheet, and Mahmoud A. Mofaddel.; project administration, Samy Bakheet and Mahmoud A. Mofaddel..; funding acquisition, Samy Bakheet and Aml El-Nagar. All authors have read and agreed to the published version of the manuscript.

## Data availability statement

The data used to support the findings of this study are available from the corresponding author upon request.

## Declaration of competing interest

The authors declare that they have no known competing financial interests or personal relationships that could have appeared to influence the work reported in this paper.

## References


[1] P. Kaur, G. Singh and P. Kaur, *Current Medical Imaging Reviews*, 14 (2018) 675-685.
[2] M. A. Albahar, *IEEE Access*, 7 (2019) 38306-38313.
[3] M. Vestergaard, P. Macaskill, P. Holt and S. Menzies, *British Journal of Dermatology*, 159 (2008) 669-676.
[4] A. Masood and A. Ali Al-Jumaily, *International Journal of Biomedical Imaging*, 2013 (2013) 1-22.
[5] W. Stolz, A. Riemann and A. Cognetta, *Eur. J. Dermatol.*, 4 (1994) 521-527.
[6] S. W. Menzies, *Dermatologic Clinics*, 19 (2001) 299-305.
[7] G. Argenziano, G. Fabbrocini, P. Carli, V. De Giorgi, E. Sammarco and M. Delfino, *Archives of Dermatology*, 134 (1998) 1563-1570.
[8] L. Song, J. Lin, Z. J. Wang and H. Wang, *IEEE Journal of Biomedical and Health Informatics*, 24 (2020) 2912-2921.
[9] S. Bakheet, *Computation*, 5 (2017) 1-13.
[10] I. Giotis, N. Molders, S. Land, M. Biehl, M. F. Jonkman and N. Petkov, *Expert Systems with Applications*, 42 (2015) 6578-6585.
[11] S. Bakheet and A. El-Nagar, *Applied Mathematics & Information Sciences*, 15 (2021) 89-96.
[12] S. Bakheet and A. Al-Hamadi, *Diagnostics*, 10 (2020) 1-15.
[13] S. Bakheet, S. Alsubai, A. El-Nagar, and A. Alqahtani, *Diagnostics*, 13 (2023) 1-16.
[14] A. Karimian, M. Ramezani and P. Moallem, *Journal of Medical Signals and Sensors*, 4 (2014) 281-290.
[15] A. N. Hoshyar, A. Al-Jumaily and A. N. Hoshyar, *Procedia Computer Science*, 42 (2014) 25-31.
[16] S. M. Jaisakthi, P. Mirunalini and C. Aravindan, *IET Computer Vision*, 12 (2018) 1088-1095.
[17] A. Victor and M. Ghalib, *International Journal of Intelligent Engineering and Systems*, 10 (2017) 444-451.
[18] M. E. Celebi, Q. Wen, H. Iyatomi, K. Shimizu, H. Zhou and G. Schaefer, *Dermoscopy Image Analysis*, 10 (2015) 97-129.
[19] T. Huang, G. Yang and G. Tang, *IEEE Transactions on Acoustics, Speech, and Signal Processing*, 27 (1979) 13-18.
[20] N. Otsu, *IEEE Transactions on Systems, Man, and Cybernetics*, 9 (1979) 62-66.
[21] L. Vincent, *Shape in Picture*, (1994) 197-208.
[22] J. Canny, *IEEE Transactions on Pattern Analysis and Machine Intelligence*, 6 (1986) 679-698.
[23] T. Ojala, M. Pietikainen and T. Maenpaa, *IEEE Transactions on Pattern Analysis and Machine Intelligence*, 24 (2002) 971-987.
[24] S. Safavian and D. Landgrebe, *IEEE Transactions on Systems, Man, and Cybernetics*, 21 (1991) 660-674.
[25] "Skin Cancer: Malignant vs. Benign|Kaggle. Available online:," [Online]. Available: https://www.kaggle.com/fanconic/skin-cancer-malignant-vsbenign. [Accessed 20 january 2023].
[26] P. Kaur, G. Singh and P. Kaur, Current Medical Imaging Reviews, 14 (2018) 675-685.
[27] A. Murugan, S. A. H. Nair, A. A. P. Preethi, and K. P. S. Kumar, *Microprocessors and Microsystems*, 81 (2021) 103727.
[28] M. A. Kassem, K. M. Hosny, and M. M. Fouad, *IEEE Access*, 8 (2020) 114822-114832.
[29] M. A. A. Thaajwer and U. A. P. Ishanka, *2nd International Conference on Advancements in Computing (ICAC)*, 1 (2020) 363-368.
[30] A. Murugan, S. A. H. Nair, and K. P. S. Kumar, *Journal of medical systems*, 43 (2019) 1-9.
[31] E. V Carrera and D. Ron-Domínguez, *4th International Conference, CITT 2018, Babahoyo, Ecuador*, (2019) 553-563.